Original Article

Elevated *MCL1* expression drives esophageal squamous cell carcinoma stemness and induces resistance to radiotherapy

Junjie Chen[1], Guoling Chen[2], Xinying Fang[2], Jie Sun[2], Jiahui Song[2], Zhiming Chen[2]

[1]Clinical Medical Research Center, Affiliated Hospital of Nantong University, Nantong, China; [2]Department of Radiotherapy & Oncology, Affiliated Hospital of Nantong University, Nantong, China

Contributions: (I) Conception and design: Z Chen; (II) Administrative support: Z Chen; (III) Provision of study materials or patients: J Chen; (IV) Collection and assembly of data: G Chen, J Song; (V) Data analysis and interpretation: X Fang, J Sun; (VI) Manuscript writing: All authors; (VII) Final approval of manuscript: All authors.

Correspondence to: Zhiming Chen, MD. Department of Radiotherapy & Oncology, Affiliated Hospital of Nantong University, No. 20 Xisi Road, Nantong 226001, China. Email: chenzhiming@ntu.edu.cn.

Background: Esophageal squamous cell carcinoma (ESCC) stands as the sixth most common cause of cancer-related mortality on a global scale, with a strikingly high proportion—over half—of these fatalities occurring within China. The emergence of radiation resistance in ESCC patients significantly diminishes overall survival rates, complicating treatment regimens and reducing clinical outcomes. There is an urgent need to explore the molecular mechanisms that underpin radiation resistance in ESCC, which could lead to the identification of new therapeutic targets aimed at overcoming this resistance. This study aims to elucidate the role of myeloid cell leukemia-1 (MCL1) in ESCC and its association with radioresistance, thereby providing a novel strategy for enhancing the efficacy of radiotherapy.

Methods: We used The Cancer Genome Atlas (TCGA) database, Genotype-Tissue Expression (GTEx) project and real-time fluorescence quantitative polymerase chain reaction (RT-qPCR) of 10 pairs of fresh endoscopic biopsy samples from patients with ESCC to analyze the messenger RNA (mRNA) expression levels of *MCL1* in esophageal cancer tissues as compared to normal tissues. Immunohistochemistry (IHC) staining and Western blotting were performed using an anti-MCL1 antibody to visualize protein expression. The mechanism of radioresistance of ESCC was examined by combining bioinformatics analysis, Western blotting, and clone formation and stemness sphere formation assays.

Results: The analysis of TCGA database and the results of RT-qPCR indicated that the mRNA level of *MCL1* was overexpressed in esophageal cancer tissues. Subsequently, the results of IHC and Western blotting showed that the protein level of MCL1 expression in cancer tissues was significantly higher than that in adjacent normal tissues. Moreover, there was a significant upregulation of *MCL1* in ESCC tissues and in radioresistant tissues and cells, with its overexpression correlating with the acquisition of stemness properties in ESCC. In terms of mechanism, *MCL1* induced cell cycle arrest by regulating the expression of *cyclin D3* and *p21* through the *JAK-STAT* signaling pathway. G0/G1 phase arrest contributed to the stem cell-like phenotype. Blocking *JAK-STAT* signaling significantly improved the efficacy of radiotherapy for ESCC.

Conclusions: These findings indicate that *MCL1* is a critical cell cycle regulator that drives the stemness and radioresistance of ESCC and may thus be a potential target in a combined therapeutic strategy aimed at overcoming radioresistance.

Keywords: Esophageal squamous cell carcinoma (ESCC); myeloid cell leukemia-1 (*MCL1*); radioresistance; stemness; cell cycle

Submitted Nov 22, 2024. Accepted for publication Dec 21, 2024. Published online Dec 28, 2024.
doi: 10.21037/jtd-2024-2027
View this article at: https://dx.doi.org/10.21037/jtd-2024-2027

Introduction

Esophageal cancer comprises two main histopathological types, esophageal squamous cell carcinoma (ESCC) and esophageal adenocarcinoma (EAC) (1), which are fundamentally different in terms of etiology and epidemiology (2,3). ESCC has an extremely strong invasive ability and is associated with a poor prognosis and a low survival rate, with its 5-year overall survival rate being approximately 17% (range, 5–34%) (4). Early ESCC is primarily treated with surgery, with surgical resection combined with perioperative radiotherapy and chemotherapy typically being applied for locally advanced ESCC (5-7). Several clinical studies on neoadjuvant chemoradiotherapy have found that patients with ESCC and pathological complete response have better long-term survival and disease-free survival rates, which are not significantly correlated with pathological type or clinical stage (8-10). Regardless of whether neoadjuvant therapy is conducted before surgery, the 5-year survival rate of patients with pathological complete response peaks at about 50%, which indicates that esophageal cancer itself varies in its sensitivity to radiotherapy and chemotherapy (11).

Radioresistance is highly common and complicates the treatment of ESCC, considerably worsening the quality of life and survival time of patients (12). Radioresistance involves cancer stem cells (CSCs), intrinsic radiation sensitivity, hypoxia-reoxygenation, cell cycle redistribution, reproliferation, repair of radiation damage, and the tumor microenvironment (13-15). Further investigation into the molecular genetics specific to ESCC is imperative, as this is crucial for gaining insights into the mechanisms underlying the onset and advancement of this disease and for devising personalized clinical treatment strategies tailored to the needs of afflicted individuals. By clarifying the genetic underpinnings of ESCC, we can enhance our understanding of the tumor's biology and thus develop more effective and targeted therapies.

In clinical practice, it has been found that some patients with ESCC experience local recurrence at the site of radiotherapy even if they have received radical surgery and adjuvant radiotherapy (16). It is reasonable to speculate that there may be some specific genetic variants that confer radioresistance in these patients with progressive ESCC, especially in those with short-term recurrence. Therefore, for this particular group of patients, it is necessary to screen and identify the related gene variants so as to guide individualized precision treatment in clinic (17-19). Whole-exome sequencing (WES) is a second-generation high-throughput sequencing technology. In the field of cancer research, it has been applied widely in examining high-frequency exon mutations and low-frequency and rarer mutations and for identifying new mutation sites (20-23). Exploiting these advances in this sequencing technology, we clarified the characteristics of gene variants in ESCC at the genomic level, identifying amplification of 1q myeloid cell leukemia-1 (*MCL1*) as a significant factor associated with progression-free survival, overall survival, and radiosensitivity in ESCC (24).

The *MCL1* gene is located on chromosome lq21 and encodes a protein with a molecular weight of 42 kD and 350 amino acids (25,26). *MCL1* amplification is found to be present in a variety of human malignancies and is dependent on the survival of many hematopoietic and other cell lines (27,28). MCL1 protein is a member of the core antiapoptotic Bcl-2 family, and MCL1 plays a role in inhibiting apoptosis by antagonizing proapoptotic Bcl-2 family proteins in mitochondria (29). Studies on ESCC, lung cancer, and other malignant tumors have demonstrated that *MCL1* contributes to drug resistance through various mechanisms, with the primary pathway being the inhibition of apoptosis (30-32). However, Lee *et al.* found that in addition to exerting an antiapoptotic effect, *MCL1* can also increase mitochondrial oxidative phosphorylation (Mt-OXPHOS), leading to the expansion of CSCs and the promotion of reactive oxygen species (ROS), with hypoxia increasing the expression of HIF-1α factor to maintain the chemoresistance of CSCs (33). Thus far, few studies have examined the role of *MCL1* in ESCC radioresistance. Only one study from Japan reported that the overexpression of

Highlight box

Key findings

- In this study, we found that myeloid cell leukemia-1 (*MCL1*) promotes the radioresistance of esophageal squamous cell carcinoma (ESCC) by enhancing stemness.

What is known and what is new?

- *MCL1* is known to participate in the regulation of ESCC radiation resistance through inhibiting apoptosis.
- In our study, *MCL1* was confirmed to enhance the radioresistance of ESCC by modulating the stemness via *JAK/STAT* signaling pathway.

What is the implication, and what should change now?

- Our research provides a potential target for combinatorial therapeutic strategy against radioresistance in the future.

SOCS1 could reverse ESCC radioresistance by inhibiting *STAT3-MCL1* axis-mediated apoptosis (34).

We thus conducted this study to clarify the function of *MCL1* in radioresistant ESCC and found that its high expression contributes to ESCC's ability to tolerate radiotherapy. The related mechanism involves the enhancement of tumor stemness via mediation of the *JAK-STAT* pathway in causing G0/G1 phase arrest. We present this article in accordance with the MDAR reporting checklist (available at https://jtd.amegroups.com/article/view/10.21037/jtd-2024-2027/rc).

Methods

Induction of radioresistant ESCC cell lines

Human esophageal endothelial cells (HEECs), and KYSE150 and ECA109 cells were purchased from Xiamen Yimo Biotechnology Co., Ltd (Xiamen, China). To develop chemotherapy-resistant variants, ECA109 and KYSE150 were cultured in RPMI-1640 medium supplemented with 10% fetal bovine serum (FBS) and 1% penicillin/streptomycin at 37 ℃ in a humidified incubator with 5% CO_2. Cells were harvested during the logarithmic growth phase and resuspended to a final concentration of 2×10^5 cells/mL. Aliquots of 100 µL were then plated into each well of a 6-well plate. After incubation for 24 hours to allow cell attachment, 2 mL of fresh RPMI-1640 medium was added to each well. The cells were then exposed to radiation therapy using a linear accelerator delivering a total dose of 36 Gy (3 fractions of 2, 4, and 6 Gy each, administered once a week). After the completion of irradiation, the cells were cultured for an additional 3 months to allow for the outgrowth of potential radioresistant clones. Cell survival was assessed using a clonogenic assay to compare the radiosensitivity of the parental cell lines with that of the irradiated cells. Surviving clones exhibiting increased radioresistance were isolated and designated as "KYSE150RR" and "ECA109RR".

Clinical samples

This study included 33 ESCC tissue samples collected from the Affiliated Hospital of Nantong University. All patients with ESCC were pathologically confirmed independently by two pathologists, and none had received any neoadjuvant radiotherapy, chemotherapy, or immunotherapy before surgery. All patients were those who received surgical operations and postoperative adjuvant radiotherapy, namely postoperative radiotherapy (PORT) patients. Patients were included and excluded based on the completeness of data, and those with complete clinical and pathological information were enrolled. All patients were followed up for at least 2 years after treatment to confirm whether local recurrence occurred. According to the local recurrence status of patients, they were divided into the recurrence group (radiotherapy-resistant group) and the stable group (radiotherapy-sensitive group). The criterion for local recurrence was that the recurrence site of the patient was the irradiated area of postoperative adjuvant radiotherapy. If a new lesion was confirmed in the relevant anatomical location by biopsy pathology, positron emission tomography/computed tomography (PET/CT) or CT, it was determined as local recurrence and classified into the radiotherapy-resistant group. If no new lesion was observed in the patient at least 2 years after treatment, they were classified into the radiotherapy-sensitive group. Finally, 23 samples were collected, including 11 cases in the radiotherapy-sensitive group and 12 cases in the radiotherapy-resistant group. The study was conducted in accordance with the Declaration of Helsinki (as revised in 2013). This study was approved by the Ethics Committee of the Affiliated Hospital of Nantong University (No. 2019-K078), and written informed consent was obtained from each patient.

Real-time fluorescence quantitative polymerase chain reaction (RT-qPCR)

RNA was isolated using TRIzol (Thermo Fisher Scientific, Waltham, MA, USA) and quantified using a NanoDrop 2000 device (Thermo Fisher Scientific). RT-qPCR was conducted as follows. The reaction system was configured with the RT-qPCR SYBR Green Kit according to the manufacturer's protocol (Vazyme Biotech Co., Ltd., Nanjing, China). The reagents in the PCR system were added to an eight-well plate, and three replicate samples were set for each sample. The plate was placed in the 7500 RT-qPCR instrument, and a total of 40 cycles were completed under the following reaction conditions: 95 ℃ for 10 minutes, 95 ℃ for 30 seconds, 59 ℃ for 32 seconds, and 72 ℃ for 31 seconds. Finally, the results were analyzed using 7500 Software v2.0 (Applied Biosystems, Thermo Fisher Scientific). PCR results were obtained after analysis of the data. The primer sequences are listed in Table S1.

Immunohistochemical (IHC) staining

For IHC staining, the tissue chip was placed in a 60 ℃ constant temperature box for baking for 2 hours. After baking, the tissue chip was placed in in xylene solution for 10 minutes, anhydrous ethanol for 5 minutes, and 95% ethanol for 5 minutes and then in 90%, 85%, and 80% ethanol for 2 minutes, respectively. Finally, the chip was rinsed with water and distilled water in a glass dish three times and finally removed. The rehydrated tissue slice was placed in citrate buffer solution and boiled at 100 ℃ for high-temperature cooking and then cooled naturally, as slicing abruptly can cause the slice to fall off, affecting the final staining effect. This process was repeated twice. After cooling, 3% hydrogen peroxide (H_2O_2) was added for 15-minute incubation, which was followed by a wash with phosphate-buffered saline (PBS) three times and a sealing with 5% bovine albumin serum (BAS) for 20 minutes; the remaining liquid was then discarded. Diluted MCL1 antibody (1:1,000) was added, and the solution was placed in a wet box at 4 ℃ overnight. Subsequently, three gentle washes with PBS buffer were performed, with each lasting 5 minutes. Secondary antibody was added, the mixture was incubated at room temperature for 30 minutes, and washed with PBS three times, after which the remaining solution was discarded. DAB chromogenic reagent was then added for color development for 5 minutes, counterstained with hematoxylin for 3 minutes, and rinsed with PBS. The slides were then mounted with gum arabic. The dyeing score was based on the number and intensity of cells with color (0–12 points). Immunological scoring was independently performed by two pathologists, and a final score was provided after discussion if there was any discrepancy.

Western blotting

For Western blotting, cell lysis solution was added after the cells were washed with PBS. The cells were lysed on a shaking table at 4 ℃ for 30 minutes. The cells were placed in a centrifuge at 4 ℃ and subjected to centrifugation at 12,000 ×g for 15 minutes for the collection of the supernatant, which was the total protein of the cells. Subsequently, 0.5 mg/mL of BSA was added in volumes of 0, 1, 2, 4, 8, 12, 16, and 20 µL to the standard protein wells, along with corresponding volumes of saline (20, 19, 18, 16, 12, 8, 4, and 0 µL), ensuring that the final volume in each well was maintained at a total of 20 µL. The protein samples were added according to the volumes of 19 µL of physiological saline and 1 µL of protein sample into protein sample wells. Based on the number of samples, bicinchoninic acid (BCA) working solution (Beyotime, Nantong, China) was prepared via the mixing of reagent A and reagent B at a ratio of 50:1, and 200 µL of this mixture was added to each well of a 96-well plate. The plate was gently shaken and incubated at 37 ℃ for 30 minutes. The absorbance (570 nm) was then measured, and a standard curve was drawn for calculating the protein concentration of each sample, with R^2>0.99 indicating a standard curve. Proteins were boiled at 100 ℃ for 5 minutes, cooled down to room temperature, and stored at –20 ℃. Sodium dodecyl sulfate-polyacrylamide gel electrophoresis (PAGE) was conducted. Protein samples were added for loading, the sample comb was removed, electrophoresis liquid was added, and 15 µL of protein was added per lane. Subsequently, 5% skim milk was used for incubation, which was performed on a shaking table at room temperature for 1 hour. Incubation with primary antibody was performed overnight at 4 ℃ on a shaking table. Horseradish peroxidase (HRP)-labeled goat anti-mouse or anti-rabbit IgG (dilution ratio of 1:1,000) was selected according to the properties of the primary antibody, with incubation occurring at room temperature on a shaking table for 1 hour. The polyvinylidene fluoride (PVDF) membrane was then washed three times with Tris-buffered saline containing Tween 20 (TBST) for 10 minutes each. As per the manufacturer's instructions for the enhanced chemiluminescence (ECL) chemiluminescence reagent kit (Sigma-Aldrich, St. Louis, MO, USA), the ECL reagent was applied evenly to the PVDF membrane. Pictures were taken using a gel imaging device to obtain immunoblotting bands. The antibodies are listed in the Table S2.

Colony formation assay

KYSE150, KYSE150RR, ECA109, and ECA109RR cells in the logarithmic growth phase were seeded into six-well plates and then treated with different doses of radiation (0, 1, 2, 4, 6, and 8 Gy). The cells were incubated at 37 ℃ for 14 days, with the medium being changed every other day. Subsequently, the cells were fixed with methanol at room temperature for 10 minutes. After being washed three times with PBS, the cells were stained with crystal violet solution for 30 minutes at room temperature. Excess crystal violet was removed, and the cells were rinsed three times with PBS.

Plasmid and small interfering RNA transfection

Cells in the logarithmic growth phase were collected by digestion and centrifugation into a 15-mL conical tube. The appropriate numbers of cells (60–70% confluence for plasmid transfection; 30–40% confluence for siRNA transfection) were then seeded into six-well plates. Two hours before transfection, the cells were placed in serum-free medium without antibiotics. Following this, 200 µL of Optimal-Minimal Essential Medium (Opti-MEM) medium and 5 µL of Lipofectamine 3000 were added to Eppendorf (EP) tube 1, and the solution was mixed gently and left to stand for 5 minutes. Subsequently, 200 µL of Opti-MEM medium and the specified amount of plasmid or siRNA were added to EP tube 2, and the solution was mixed gently and let stand for 5 minutes. The contents of EP tubes 1 and 2 were combined, incubated for 20 minutes, and then added to the corresponding wells of the six-well plate. Forty-eight hours later, RNA or proteins were collected for subsequent analysis.

Cell cycle analysis

For the analysis of the cell cycle, cells were seeded in six-well plates at a density of 1×10^6 cells per well and incubated overnight. After a wash with PBS, they were fixed using 70% ice-cold ethanol and stored at 4 ℃ overnight. The cells were then washed again and resuspended in PBS before being treated with RNase A (20 µg/mL) and propidium iodide (PI) (50 µg/mL), which was followed by incubation at 37 ℃ for 30 minutes. Subsequently, flow cytometry analysis was performed using a flow cytometer (Beckman Coulter, Brea, CA, USA). CellQuest software was used to manually define regions corresponding to the G0/G1, S, and G2/M phases for cell cycle assessment. Each treatment group underwent three independent experiments. Flow cytometric data for DNA cell cycle analysis was processed using FlowJo software (FlowJo, Ashland, OR, USA).

Sphere formation assay

The cells in the logarithmic growth phase were digested, centrifuged, collected, and washed twice with PBS. After culture, the cells were resuspended at 1,000 cells/100 µL and inoculated in a U-shaped low-adsorption 96-well plate. After adherence, the cells were irradiated (9 Gy) and cultured in a 37 ℃, 5% CO_2 incubator. After 2 weeks of incubation, the sphere formation of the cells was photographed under the microscope and quantified.

Bioinformatics analysis

The databases based on The Cancer Genome Atlas (TCGA) database and Genotype-Tissue Expression (GTEx) project were used to analyze the expression of *MCL1* in ESCC (https://xenabrowser.net/hub/). We used esophageal cancer samples from TCGA database and divided them into high- and low-expression groups based on the median *MCL1* expression levels. We then performed differential gene analysis between the two groups, defining genes with |log fold change (FC)| >1 and an adjusted P value <0.05 as differentially expressed genes. Using the clusterProfiler package, we conducted Kyoto Encyclopedia of Genes and Genomes (KEGG) pathway analysis on these differentially expressed genes, visualizing the top 15 significantly enriched pathways. Subsequently, we performed gene set enrichment analysis (GSEA) using the "clusterProfiler" package in R with the entire set of genes, sorting them by logFC. The *JAK-STAT3* pathway genes identified by GSEA (http://www.gsea-msigdb.org/), stemness related genes reported in literature and *MCL1* were uploaded to the Search Tool for Retrieval of Interacting Genes/Proteins (STRING) website for network interaction analysis. The minimum required interaction score was set to 0.4, and nodes without connections were not removed. Using cytoHubba within the Cytoscape software, we identified the hub genes among the top 25 genes using the EcCentricity algorithm and selecting the top 10 nodes.

Statistical analysis

All experiments were performed in triplicate. The data analysis and data graphs were completed using GraphPad Prism 8.0 (GraphPad Software, La Jolla, CA, USA) and SPSS 23 software (IBM Corp., Armonk, NY, USA). The differences between groups were analyzed with the *t* test, and the differences between multiple groups were analyzed with one-way analysis of variance (ANOVA). The hypothesis test level was set at $\alpha=0.05$, and $P<0.05$ was considered to indicate statistical significance.

Results

The messenger RNA (mRNA) and protein expressions of MCL1 were significantly higher in ESCC tumor tissues and cell lines compared than in normal tissue and cells

To investigate the relationship between *MCL1* and ESCC, we initially used TCGA database and GTEx project to

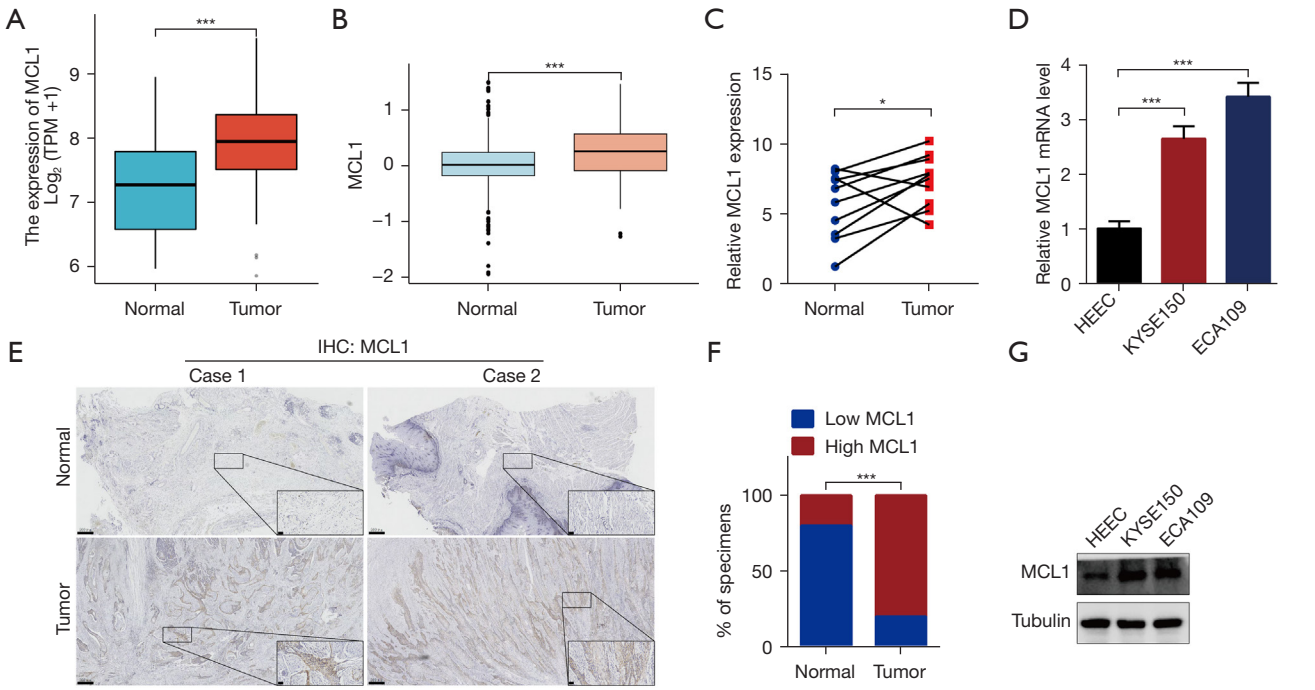

Figure 1 The mRNA and protein expressions of *MCL1* were higher in esophageal cancer tissues and cell lines than those in normal tissues and cells. (A) TCGA database was used to analyze the expression of *MCL1* mRNA in unpaired samples of patients with esophageal cancer. (B) TCGA database and GTEx project were used to analyze the expression of *MCL1* mRNA in tissues. (C) RT-qPCR was used to detect *MCL1* mRNA expression in 10 pairs of fresh esophageal cancer tissues and adjacent tissues. (D) RT-qPCR was used to detect *MCL1* mRNA expression in normal esophageal epithelial cells and esophageal cancer cell lines. (E) Immunohistochemistry was used to detect the expression of MCL1 in 10 paired esophageal cancer tissues. Representative images are shown. Scale bars: 500 μm (original image), 50 μm (enlarged image). (F) Immunohistochemical score of MCL1 expression level. (G) Western blotting of MCL1 protein expression in human normal esophageal epithelial cell lines and esophageal cancer cell lines. *, P<0.05; ***, P<0.001. *MCL1*, myeloid cell leukemia-1; TPM, transcripts per million; IHC, immunohistochemistry; TCGA, The Cancer Genome Atlas; GTEx, Genotype-Tissue Expression; RT-qPCR, real-time fluorescence quantitative polymerase chain reaction.

analyze *MCL1* transcription. The results revealed that the transcriptional level of *MCL1* was significantly higher in tumor tissues compared to normal tissue (*Figure 1A*,*1B*). Additionally, RT-qPCR analysis of 10 fresh surgical samples from patients with ESCC showed an obvious increase in *MCL1* transcriptional expression levels in tumor tissue (*Figure 1C*). Furthermore, RT-qPCR analysis also demonstrated that the mRNA expression of *MCL1* was significantly higher in ESCC cell lines than in human normal esophageal epithelial cells (*Figure 1D*).

Next, to determine the protein expression of MCL1 in ESCC tissue samples, we initially collected 10 patient samples for IHC analysis. The findings revealed positive cytoplasmic and nuclear expression of MCL1 protein, indicated by brown particles (*Figure 1E*). Moreover, in 80% (8/10) of the ESCC tissues examined, MCL1 protein expression was higher compared to that of the corresponding normal tissue (*Figure 1F*). Western blotting results further indicated significantly elevated levels of MCL1 protein in ESCC cell lines KYSE150 and ECA109 as compared to normal HEECs (*Figure 1G*). These outcomes strongly suggest that *MCL1* may play a crucial role in the development of ESCC.

MCL1 protein expression was significantly increased in patients with ESCC with radioresistance

To explore the multifaceted role of *MCL1* in the progression of ESCC beyond its established association with esophageal malignancies, we conducted an exhaustive WES analysis on a cohort of 23 previously gathered ESCC specimens. Our previously findings revealed that gains in chromosome 1q

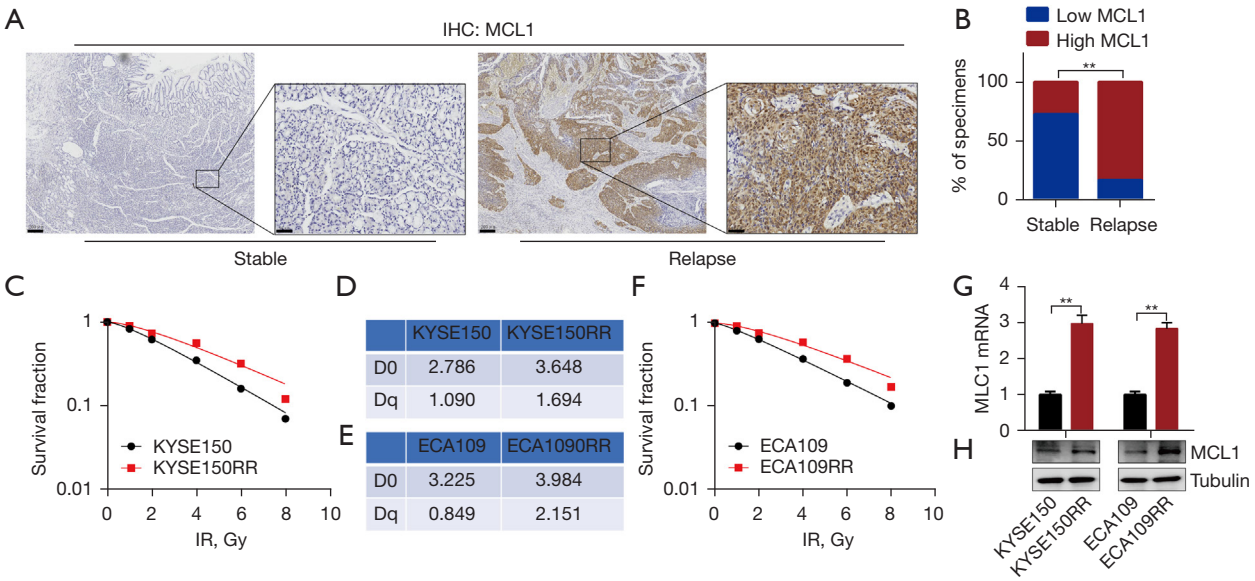

Figure 2 MCL1 protein expression was significantly increased in patients with ESCC and radioresistance. (A) Immunohistochemical analysis of the MCL1 expression of 23 patients with esophageal carcinoma tissues. Representative images are shown. Scale bars: 200 μm (original image), 50 μm (enlarged image). (B) Quantification of MCL1 expression according to immunohistochemical score. (C,D) Survival curves, mean lethal dose (D0), and quasithreshold dose (Dq) of KYSE150 cells and their corresponding resistant cell lines after different doses of irradiation. (E,F) Survival curves, D0, and Dq of esophageal cancer cell line ECA109 and its corresponding resistant cell line after irradiation with different doses. (G) RT-qPCR was used to detect the transcriptional expression of MCL1 in esophageal cancer cell lines. (H) The expression of MCL1 protein in different esophageal cancer cell lines was detected by Western blotting. **, P<0.01. IHC, immunohistochemistry; *MCL1*, myeloid cell leukemia-1; IR, X-ray irradiation; RR, radiation resistance; ESCC, esophageal squamous cell carcinoma; RT-qPCR, real-time fluorescence quantitative polymerase chain reaction.

copy number were significantly linked to an elevated risk of tumor recurrence following radiotherapy in patients with esophageal cancer. Notably, the *MCL1* gene, located on chromosome 1q, exhibited amplification in these samples, suggesting a potential mechanistic link between *MCL1* overexpression and radioresistance (24). To further substantiate this connection at the protein level, IHC was employed to assess MCL1 expression in the aforementioned ESCC tissues. Our results demonstrated a pronounced upregulation of *MCL1* in the tissue samples from patients who experienced recurrence postradiotherapy. Specifically, within the recurrent group, a remarkable 83.3% (10 out of 12) of cases displayed heightened MCL1 protein expression, a stark contrast to the 27.3% (3 out of 11) observed in the stable disease group (*Figure 2A*,*2B*). These data collectively implicate *MCL1* as a pivotal player in modulating the radiosensitivity of ESCC and thus potentially serving as a biomarker for predicting treatment outcomes and guiding therapeutic strategies.

To confirm the involvement of *MCL1* in ESCC radiation resistance, we engineered radiation-resistant ESCC cell lines. Through a series of cloning experiments, we validated the establishment of these resistant strains. A clonogenic survival assay was used to delineate cell survival curves, enabling us to quantify the average lethal dose (D0) and subthreshold dose (Dq) parameters. Our analyses revealed a notable elevation in the survival fraction, D0, and Dq values after radiation induction, indicative of an acquired resistance to radiotherapy (*Figure 2C-2F*). The resistant cells were named "KYSE150RR" and "ECA109RR".

RT-qPCR assay was used to detect the transcription of *MCL1* in the parental and radioresistant ESCC cells. The results showed that the transcription level of *MCL1* in the resistant cell line was significantly higher than that in the parental cell line (*Figure 2G*). Western blotting analysis of MCL1 protein expression showed that the expression of MCL1 protein in the resistant cell line was significantly higher than that in the parental cell line (*Figure 2H*).

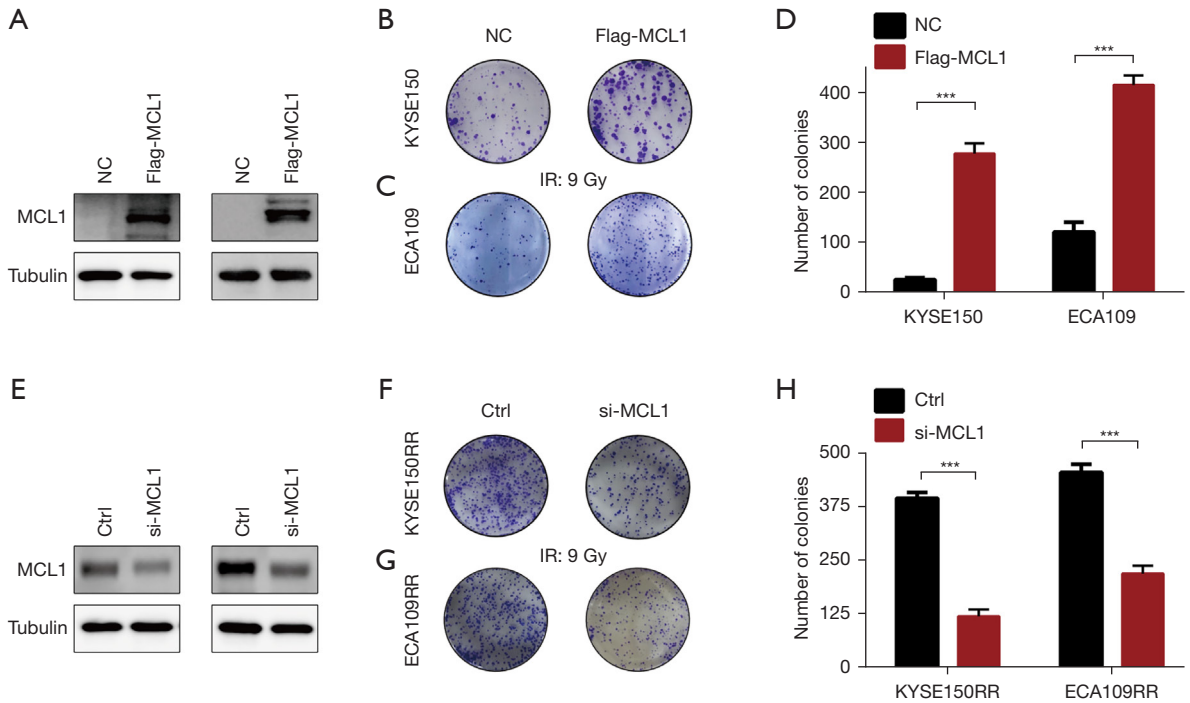

Figure 3 *In vitro MCL1* overexpression enhanced the radiotherapy resistance of ESCC. (A) NC and *MCL1*-overexpression (Flag-MCL1) plasmid were transfected into parental cell lines, and the transfection effect was detected via Western blotting. (B-D) Cells were exposed to X-ray irradiation and then subjected to a colony formation assay. After 14 days, the colonies were fixed with methanol, stained with crystal violet, and counted. (E) Control (Ctrl) and *MCL1* siRNA (si-MCL1) was transfected into radioresistant cell lines, and the transfection effect was detected via Western blotting. (F-H) Cells were exposed to X-ray irradiation and then subjected to a colony formation assay. After 14 days, the colonies were fixed with methanol, stained with crystal violet, and counted. ***, P<0.001. *MCL1*, myeloid cell leukemia-1; NC, normal control; IR, X-ray irradiation; RR, radiation resistance; ESCC, esophageal squamous cell carcinoma.

MCL1 overexpression enhanced radiotherapy resistance of ESCC in vitro

In the parental cell lines KYSE150 and ECA109, MCL1 overexpression promoted the proliferation of cells, as indicated by colony formation assay (*Figure 3A-3D*). In contrast, MCL1 was knocked down in the KYSE150RR and ECA109RR cell lines (*Figure 3E*). The results of colony formation assay showed that the proliferation ability of radio-resistant cell lines was significantly reduced by MCL1 knockdown (*Figure 3F-3H*).

MCL1 may regulate the stemness of ESCC through the JAK-STAT pathway

In order to further clarify the molecular mechanism underlying the involvement of *MCL1* in the radiosensitivity of ESCC, we performed chemical and genetic perturbation based on the esophageal cancer data of TCGA database. Among the KEGG datasets analyzed, 15 signaling pathways emerged as significantly enriched based on stringent P value thresholds. Notably, *MCL1* was prominently associated with the cell cycle and the *JAK-STAT* signaling pathway (*Figure 4A*), underscoring its potential role in these critical biological processes. The GSEA results showed that pathways related to tumor stemness were significantly enriched in the high-*MCL1* expression group, including the *STEM CELL UP* and *CELL_CYCLE* terms (*Figure 4B*,*4C*).

Using cytoHubba within the Cytoscape software and the STRING database (https://cn.string-db.org/), we identified *MCL1* as a hub gene within this network (*Figure 4D*). TCGA database was used to analyze the correlation between these genes and *MCL1*, and the results showed that *MCL1* was significantly positively correlated with *JAK1-3*, *STAT1/3/5B*, *MYC*, and *SNAI1* (*Figure 4E*). In ESCC cell lines, overexpression of *MCL1* led to a significant upregulation in the expression of *STAT3*, *SNAI1*, *CD44* and *MYC*

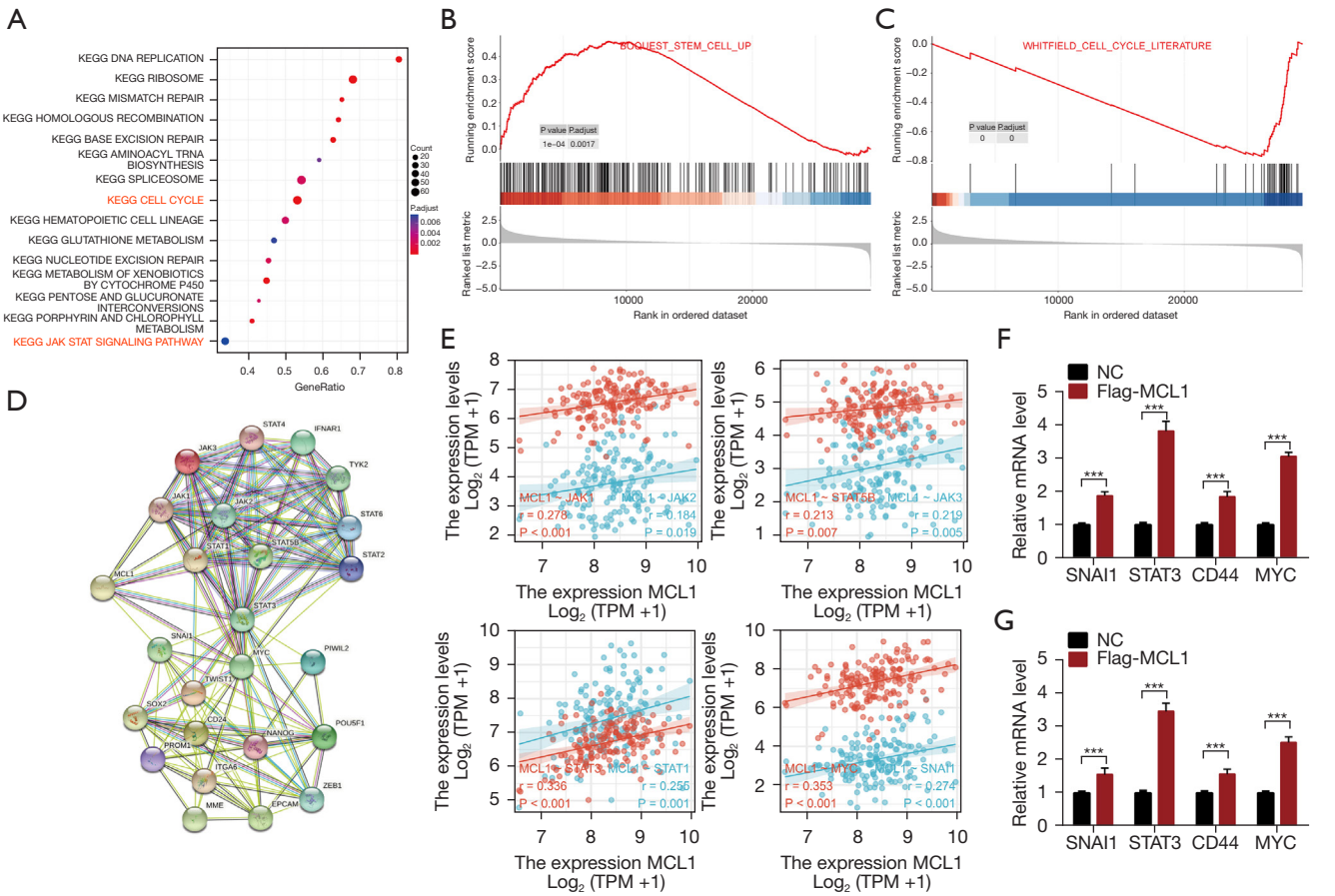

Figure 4 GSEA of esophageal cancer using TCGA data indicated that *MCL1* may regulate the stemness of esophageal cancer through the *JAK-STAT* pathway. (A) TCGA database was used to perform GSEA pathway enrichment analysis with the KEGG pathway database as the background, and the 15 pathways with the most significant P values were visualized. (B) Pathway GSEA of the correlation between *MCL1* and cell stemness. (C) The correlation between *MCL1* and cell cycle was analyzed via GSEA pathway enrichment. (D) The STRING database was used to analyze the protein interaction between *MCL1* and the *JAK-STAT* pathway and stemness-related genes. (E) TCGA database was used to analyze the correlation between *MCL1* and the *JAK-STAT* pathway and stemness-related gene transcription levels. (F,G) Normal control (NC) and *MCL1*-overexpression (Flag-MCL1) plasmid were transfected into ECA109 and KYSE150 cells, and the transcriptional expression of *STAT3*, *SNAI1*, CD44 and *MYC* was detected. ***, P<0.001. TPM, transcripts per million; *MCL1*, myeloid cell leukemia-1; JAK, janus kinase; STAT, signal transducer and activator of transcription; KEGG, Kyoto Encyclopedia of Genes and Genomes; *SNAI1*, snail family transcriptional repressor 1; *MYC*, MYC proto-oncogene, BHLH, transcription factor; GSEA, gene set enrichment analysis; TCGA, The Cancer Genome Atlas.

(*Figure 4F,4G*). These findings collectively suggest a mechanistic link between *MCL1* and the modulation of CSC properties and cell cycle regulation in ESCC.

MCL1 promoted G0/G1 phase arrest by regulating the expression of cyclin D3 and p21

Studies have confirmed that there is a close relationship between cell G0/G1 phase arrest and tumor cell stemness, and *MCL1* has been confirmed to be an antiapoptotic protein (14,29). To determine the effect of *MCL1* on cell cycle, flow cytometry analysis was performed. The results showed that overexpression of MCL1 induced significant G0/G1 phase arrest in KYSE150 and ECA109 cells (*Figure 5A,5B*). Furthermore, Western blotting showed that overexpression of MCL1 increased the expression of the inhibitory cyclin p21 and decreased the expression of cyclin D3, a key protein in the regulation of G1-to-S phase

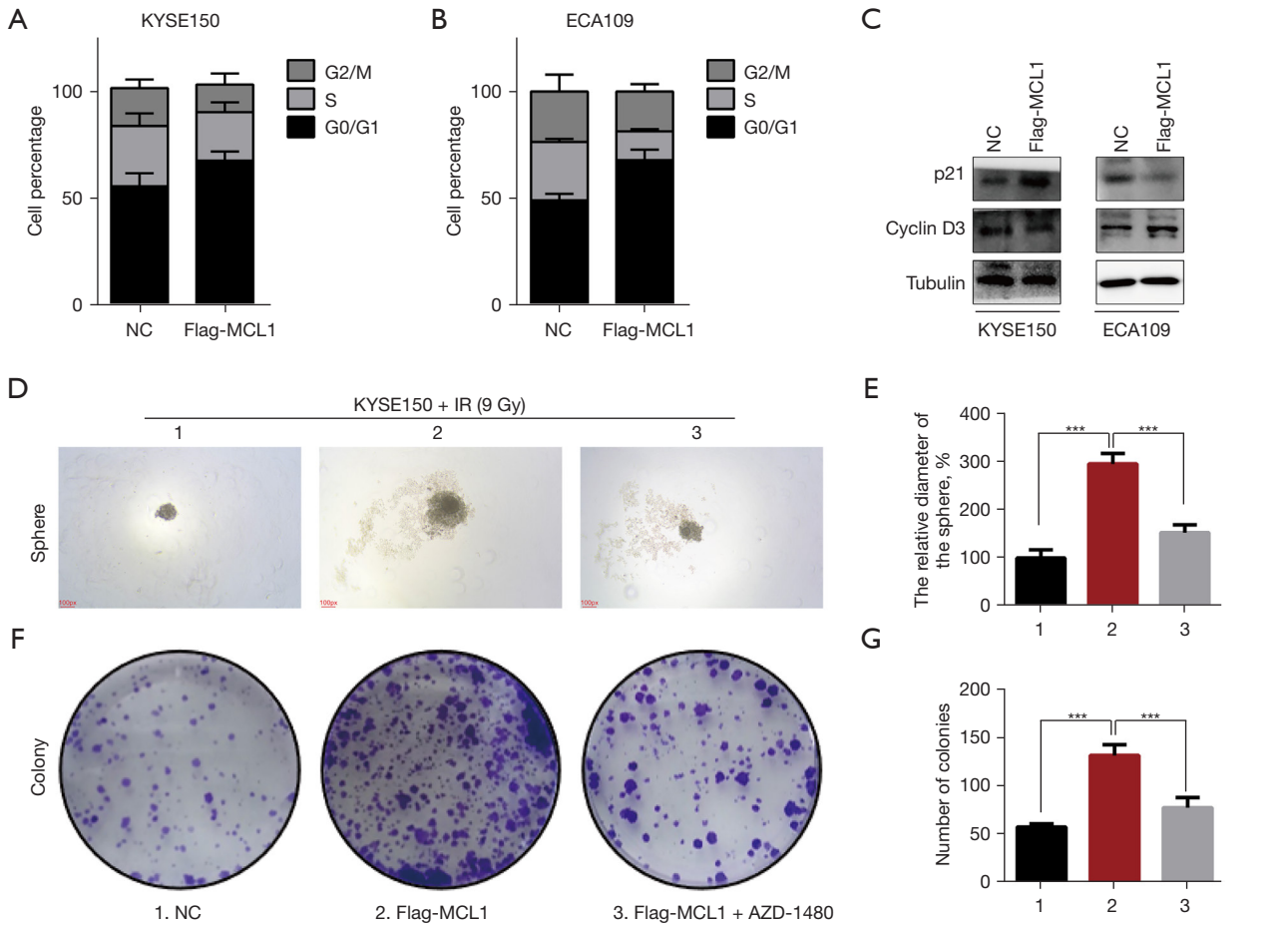

Figure 5 *MCL1* regulated cell G0/G1 phase arrest by regulating cyclin D3 and p21 expression. (A,B) After NC and *MCL1*-overexpression (Flag-MCL1) plasmid was transfected into in KYSE150 and ECA109 cells, cell cycle changes were detected via flow cytometry. (C) *MCL1* was overexpressed in the cells, and cyclin D3 and p21 protein expression was detected by Western blotting. (D,E) Stemness sphere formation assay was performed with transfected cells or with inhibitors, and the cells were observed under microscopy after 14 days. (F,G) Cell clonogenic assays were performed on cell lines treated with transfection or combined inhibitors, and 14 days later, the cells were fixed with methanol for 30 minutes, stained with crystal violet for 30 minutes, and then counted. ***, P<0.001; 1, NC; 2, Flag-MCL1; 3, Flag-MCL1 + AZD-1480; NC, normal control; *MCL1*, myeloid cell leukemia-1; IR, X-ray irradiation.

transition (*Figure 5C*). MCL1 could regulate cell cycle arrest in the G0/G1 phase via cyclin D3 and p21.

To elucidate the role of the *JAK-STAT* pathway in the *MCL1*-mediated radiotherapy resistance of esophageal cancer, we employed the well-characterized *JAK* inhibitor, AZD-1480, in our cellular models. This intervention was designed to evaluate the impact of *MCL1* impact on *JAK* signaling dynamics and its downstream effects on tumor biology. Our findings revealed that enforced *MCL1* expression significantly augmented the tumorigenic potential of esophageal cancer cells, which manifested as an enhanced sphere-forming capacity and radioresistance. Intriguingly, treatment with AZD-1480 effectively abrogated the radioprotective effect conferred by *MCL1* overexpression, reestablishing cellular sensitivity to radiotherapy (*Figure 5D-5G*). These data collectively support the notion that *MCL1* operates as a critical regulator of tumor stem cell traits and radioresistance, exerting its influence, at least in part, through the modulation of the *JAK-STAT* signaling cascade. This study underscores the potential of targeting *MCL1* and its associated pathways as a viable strategy for overcoming radiotherapy resistance in esophageal cancer, offering new

avenues for therapeutic intervention.

Discussion

MCL1 was first discovered in 1993, being initially identified by Craig and colleagues as an up-regulated gene in the early differentiation of human myeloid leukemia cells (35). As a member of the antiapoptotic *Bcl-2* family, *MCL1* prevents the proapoptotic proteins *Bcl-2* homologous antagonistic killer protein (*Bak*) and *Bcl-2*-associated protein X (*Bax*) from forming pores in the mitochondrial membrane such that cytochrome C is not released into the cytoplasm (36,37). *MCL1* also inhibits the cysteine protease family, reducing subsequent caspase activation, which is primarily responsible for the degradation of most large molecules during apoptosis (38). *MCL1* has a broad but specialized tissue distribution and has been shown to be involved in the survival and development of multiple cell types (39-42). In addition to its role in apoptosis and differentiation, *MCL1* is also known to influence cell cycle progression (43,44). Beroukhim *et al.* and Wang *et al.* performed extensive somatic copy number amplification (SCNA) genomic analysis on more than 3,000 cancer specimens representing 26 histological types and found that *MCL1* was enriched in focal SCNA regions; moreover, *MCL1* amplification was found in cancers of a variety of tissue types, including breast cancer, lung adenocarcinoma, and melanoma (28,45). *MCL1* expression often appears in a wide variety of tumor types and is closely associated with the poor prognosis of patients and the drug resistance of tumors (25,46-48). The second-generation *MCL1* antagonists may be key targets for cancer treatment (49-51). In esophageal cancer, the *MCL1* inhibitor obatoclax can significantly reduce the expression of multidrug resistance gene 1 (*MDR1*) and overcome the resistance of ESCC to cisplatin through the *Src-MCL1-MDR1* pathway (31). However, thus far, few studies on *MCL1* amplification and ESCC radiotherapy resistance have been conducted.

In the first part of this study, WES-sequencing technology was used to compare the genetic information of patients with ESCC with differing prognoses after postoperative radiotherapy, and several genetic variants including *MCL1* amplification were found to be associated with radiotherapy resistance. We further aimed to investigate the role and mechanism of *MCL1* in ESCC radioresistance. Initially, we established the relationship between *MCL1* and ESCC through an analysis of TCGA database, followed by validation using 10 fresh surgical samples from patients with ESCC. The results showed that the transcriptional level of *MCL1* in ESCC tissues was significantly higher than that in adjacent normal tissues. Subsequently, we investigated and analyzed the relationship between *MCL1* expression and sensitivity to radiotherapy as well as radiation resistance. The results indicated that MCL1 expression was significantly elevated in patients exhibiting radiation resistance compared to those demonstrating radiation sensitivity, which aligns with the existing literature on *MCL1* expression in ESCC (31,32,34). Among the Bcl-2 family members, the antiapoptotic protein MCL1 has a short half-life, which makes this protein highly sensitive to changes in synthesis or degradation; therefore, examining *MCL1* regulators can help to uncover the mechanism of disease development and treatment (52). In the subsequent validation experiments, we also found that the expression of *MCL1* was significantly higher in the radioresistant ESCC cell lines than in their parental cell lines. In the *in vitro* cell model experiment, overexpression of *MCL1* in the KYSE150 and ECA109 cell lines significantly increased the radioresistance of ESCC cells, suggesting that *MCL1* overexpression promotes the radioresistance of ESCC cells. The cloning experiment confirmed that the resistance of KYSE150RR and ECA109RR cells to radiation was significantly reduced after *MCL1* was knocked down. The above results confirm that MCL1 participates in regulating the radiation resistance of ESCC, which is consistent with the research results of Sugase *et al.* (34). Taken together, the above results suggest that MCL1 may be involved in the radiosensitivity of ESCC.

The ultimate goal of gene sequencing analysis is to characterize gene expression patterns, facilitate a more in-depth interpretation of the results to clarify the biological mechanisms, and according to the differentially expressed genes between different categories, extract significant and meaningful results. With the widespread application of high-throughput sequencing technologies, increasingly larger datasets that are difficult to analyze and integrate have been generated, but traditional gene expression analysis strategies focus on identifying individual genes that exhibit differences between two states, which while useful, cannot clarify the related biological processes such as metabolic pathways, transcriptional programs, and stress responses (53). These biological processes are distributed in the whole gene network, but they are indiscernible when examined at the level of a single gene, so it is difficult for traditional gene analysis methods to generate meaningful conclusion from these data. GSEA, first proposed by the Broad

Institute, is a powerful enrichment analysis tool. Compared with the single-gene methods, GSEA has three main advantages: First, it by identifying pathways and processes to simplify the interpretation of the large-scale experiments, researchers can focus on gene sets rather than on the genes with high scores, as gene sets tend to be easier to copy and thus more interpretable. Second, GSEA can help highlight true biological signals amid background noise. In a set of strongly correlated genes, even if the changes in individual genes are modest, GSEA can enhance the signal by integrating the overall changes, thus improving the effectiveness of the analysis. Third, this analysis can help define gene subgroups to elucidate the results (54). Therefore, GSEA has now become an integral part of high-throughput gene expression data analysis and is an algorithm widely used to identify statistically rich gene sets in transcriptome data. KEGG is a knowledge base that links genomic information with higher-order functional information and can be used for the systematic analysis of gene functions (55). Genomic information is stored in the gene database, which is a collection of gene catalogues of all fully sequenced genomes and partial genomes with up-to-date annotations of gene function. Higher-order functional information is stored in the KEGG PATHWAY database, which contains graphical representations of cellular processes such as metabolism, membrane transport, signal transduction, and cell cycle. Its purpose is to facilitate the use of computers to achieve a comprehensive display of the biological information contained in cells and organisms. With this genomic information, computing can calculate or predict complex pathways in cells or biologically complex behavior. In this study, *MCL1* was found to be significantly correlated with KEGG terms "cell cycle" and "*JAK-STAT* signaling pathway". In addition, GSEA showed that *MCL1* had a positive correlation with tumor stemness but a negative correlation with cell cycle arrest. Overall, the GSEA findings suggest that the radioresistance of *MCL1* in ESCC may be related to the *JAK–STAT* pathway, stemness-related genes, and cell cycle arrest.

The purpose of the STRING database is integrate all known and predicted associations between proteins, including physical interactions and functional associations (56). In this study, the STRING database was used to analyze the protein interaction between *MCL1* and the *JAK-STAT* pathway and stemness-related genes, and it was found that *MCL1* was closely related to *JAK-STAT* and stemness. TCGA database was used to analyze the correlation between *MCL1* and the *JAK-STAT* pathway and stemness-related gene transcription levels. ECA109 and KYSE150 cells overexpressing *MCL1* were used to detect the transcriptional expression of *JAK1*, *STAT1*, *SNAI1* and *MYC*, and the results showed that *MCL1* was positively correlated with *JAK1-3*, *STAT1/3/5B*, *MYC*, and *SNAI1*. In the subsequent cell experiments, *JAK1*, *STAT1*, *OCT4*, and *SNAI1* were indeed significantly upregulated after the overexpression of *MCL1* in esophageal cancer cell lines, which was consistent with the results of TCGA database analysis. In addition, a large number of studies have confirmed that cell cycle arrest is closely related to tumor cell stemness (57-59). We overexpressed *MCL1* in KYSE150 cells and detected cell cycle changes via flow cytometry, and the results showed that overexpression of *MCL1* could cause significant G0/G1 phase arrest in KYSE150 cells. Therefore, these results suggest that overexpression of *MCL1* promotes stemness gene expression in ESCC.

Finally, to understand the importance of the *JAK-STAT* pathway in the *MCL1*-mediated radioresistance of esophageal cancer, we first used the previously documented *JAK-STAT* inhibitor AZD-1480 in immunoblotting analysis for experimental confirmation (60). After overexpression of *MCL1*, the protein levels of *OCT-4* and *SNAI1* were significantly upregulated, while the upregulation effect was significantly weakened after cotreatment with AZD-1480. Clonogenic assay showed that AZD-1480 reversed the effect of *MCL1* overexpression on the radioresistance of tumor cells. Therefore, these results suggest that *MCL1* promotes radioresistance by regulating tumor stemness through the *JAK–STAT* pathway.

Conclusions

In conclusion, the expression of *MCL1* was detected at both the mRNA and protein level in 10 pairs of fresh surgical specimens from patients with ESCC and 23 pairs of ESCC tissues and adjacent normal tissues via RT-qPCR, Western blotting, and IHC. These experiments suggested that *MCL1* was associated with the radiosensitivity of ESCC. The role of *MCL1* in radioresistance of ESCC was further confirmed by knockdown or overexpression of *MCL1* in the parental and radioresistant ESCC cell lines. Finally, TCGA database was used to perform GSEA and KEGG, STRING database analysis, and related verification experiments. *MCL1* enhances the radioresistance of ESCC by promoting the expression of stem-related genes including *JAK1*, *STAT1*, *OCT4*, and *SNAI1*, as well as the tumor stemness mediated by the *JAK-STAT* pathway.

Acknowledgments

We would like to thank Qin Jin for helping with the analysis of pathological sections.

Funding: This work was supported by grants from the Research Project of Nantong Health Committee (No. MS2023008), the National Natural Science Foundation of China (No. 82203096), the Chinese Postdoctoral Science Foundation (No. 2022M711717), and the Jiangsu Provincial Research Hospital (No. YJXYY202204-YSB27).

Footnote

Reporting Checklist: The authors have completed the MDAR reporting checklist. Available at https://jtd.amegroups.com/article/view/10.21037/jtd-2024-2027/rc

Data Sharing Statement: Available at https://jtd.amegroups.com/article/view/10.21037/jtd-2024-2027/dss

Peer Review File: Available at https://jtd.amegroups.com/article/view/10.21037/jtd-2024-2027/prf

Conflicts of Interest: All authors have completed the ICMJE uniform disclosure form (available at https://jtd.amegroups.com/article/view/10.21037/jtd-2024-2027/coif). The authors have no conflicts of interest to declare.

Ethical Statement: The authors are accountable for all aspects of the work in ensuring that questions related to the accuracy or integrity of any part of the work are appropriately investigated and resolved. The study was conducted in accordance with the Declaration of Helsinki (as revised in 2013). Ethical approval was obtained from Ethics Committee of Affiliated Hospital of Nantong University (No. 2019-K078), and written informed consent was obtained from each patient.

References

1. Strzelec B, Chmielewski PP, Kielan W. Esophageal cancer: current status and new insights from inflammatory markers - a brief review. Pol Przegl Chir 2024;96:83-7.
2. Harada K, Rogers JE, Iwatsuki M, et al. Recent advances in treating oesophageal cancer. F1000Res 2020;9:F1000 Faculty Rev-1189.
3. Deboever N, Jones CM, Yamashita K, et al. Advances in diagnosis and management of cancer of the esophagus. BMJ 2024;385:e074962.
4. Rustgi AK, El-Serag HB. Esophageal carcinoma. N Engl J Med 2014;371:2499-509.
5. Mariette C, Piessen G, Triboulet JP. Therapeutic strategies in oesophageal carcinoma: role of surgery and other modalities. Lancet Oncol 2007;8:545-53.
6. Ilson DH, van Hillegersberg R. Management of Patients With Adenocarcinoma or Squamous Cancer of the Esophagus. Gastroenterology 2018;154:437-51.
7. Yang H, Liu H, Chen Y, et al. Neoadjuvant Chemoradiotherapy Followed by Surgery Versus Surgery Alone for Locally Advanced Squamous Cell Carcinoma of the Esophagus (NEOCRTEC5010): A Phase III Multicenter, Randomized, Open-Label Clinical Trial. J Clin Oncol 2018;36:2796-803.
8. Urba SG, Orringer MB, Turrisi A, et al. Randomized trial of preoperative chemoradiation versus surgery alone in patients with locoregional esophageal carcinoma. J Clin Oncol 2001;19:305-13.
9. Kleinberg L, Knisely JP, Heitmiller R, et al. Mature survival results with preoperative cisplatin, protracted infusion 5-fluorouracil, and 44-Gy radiotherapy for esophageal cancer. Int J Radiat Oncol Biol Phys 2003;56:328-34.
10. Chirieac LR, Swisher SG, Ajani JA, et al. Posttherapy pathologic stage predicts survival in patients with esophageal carcinoma receiving preoperative chemoradiation. Cancer 2005;103:1347-55.
11. Loew A, Schneider C, Pflüger M, et al. Treatment reality of esophageal cancer in the Federal State of Brandenburg : Comparison between squamous cell carcinoma and adenocarcinoma. Chirurgie (Heidelb) 2024;95:825-32.
12. Li X, Liu H, Gao W, et al. Octadecyl Gallate and Lipid-Modified MnSe(2) Nanoparticles Enhance Radiosensitivity in Esophageal Squamous Cell Carcinoma and Promote Radioprotection in Normal Tissues. Adv Mater 2024;36:e2311291.

13. Baumann M, Krause M, Overgaard J, et al. Radiation oncology in the era of precision medicine. Nat Rev Cancer 2016;16:234-49.
14. Schulz A, Meyer F, Dubrovska A, et al. Cancer Stem Cells and Radioresistance: DNA Repair and Beyond. Cancers (Basel) 2019;11:862.
15. Yang Q, Gao W, Li X, et al. Targeting ABCA1 via Extracellular Vesicle-Encapsulated Staurosporine as a Therapeutic Strategy to Enhance Radiosensitivity. Adv Healthc Mater 2024;13:e2400381.
16. Ma GF, Lin GL, Wang ST, et al. Prediction of recurrence-related factors for patients with early-stage cervical cancer following radical hysterectomy and adjuvant radiotherapy. BMC Womens Health 2024;24:81.
17. Qin HD, Liao XY, Chen YB, et al. Genomic Characterization of Esophageal Squamous Cell Carcinoma Reveals Critical Genes Underlying Tumorigenesis and Poor Prognosis. Am J Hum Genet 2016;98:709-27.
18. Lin DC, Hao JJ, Nagata Y, et al. Genomic and molecular characterization of esophageal squamous cell carcinoma. Nat Genet 2014;46:467-73.
19. Gao YB, Chen ZL, Li JG, et al. Genetic landscape of esophageal squamous cell carcinoma. Nat Genet 2014;46:1097-102.
20. Forouzanfar N, Baranova A, Milanizadeh S, et al. Novel candidate genes may be possible predisposing factors revealed by whole exome sequencing in familial esophageal squamous cell carcinoma. Tumour Biol 2017;39:1010428317699115.
21. Dai W, Ko JMY, Choi SSA, et al. Whole-exome sequencing reveals critical genes underlying metastasis in oesophageal squamous cell carcinoma. J Pathol 2017;242:500-10.
22. Lin DC, Dinh HQ, Xie JJ, et al. Identification of distinct mutational patterns and new driver genes in oesophageal squamous cell carcinomas and adenocarcinomas. Gut 2018;67:1769-79.
23. Weng Z, Mai Z, Yuan J, et al. Evolution of genome and immunogenome in esophageal squamous cell carcinomas driven by neoadjuvant chemoradiotherapy. Int J Cancer 2024;155:2021-35.
24. Chen Z, Yao N, Zhang S, et al. Identification of critical radioresistance genes in esophageal squamous cell carcinoma by whole-exome sequencing. Ann Transl Med 2020;8:998.
25. Montalban-Bravo G, Thongon N, Rodriguez-Sevilla JJ, et al. Targeting MCL1-driven anti-apoptotic pathways overcomes blast progression after hypomethylating agent failure in chronic myelomonocytic leukemia. Cell Rep Med 2024;5:101585.
26. Mukherjee N, Katsnelson E, Brunetti TM, et al. MCL1 inhibition targets Myeloid Derived Suppressors Cells, promotes antitumor immunity and enhances the efficacy of immune checkpoint blockade. Cell Death Dis 2024;15:198.
27. Andersen JL, Kornbluth S. Mcl-1 rescues a glitch in the matrix. Nat Cell Biol 2012;14:563-5.
28. Beroukhim R, Mermel CH, Porter D, et al. The landscape of somatic copy-number alteration across human cancers. Nature 2010;463:899-905.
29. Duan L, Tadi MJ, O'Hara KM, et al. Novel markers of MCL1 inhibitor sensitivity in triple-negative breast cancer cells. J Biol Chem 2024;300:107375.
30. Whitsett TG, Mathews IT, Cardone MH, et al. Mcl-1 mediates TWEAK/Fn14-induced non-small cell lung cancer survival and therapeutic response. Mol Cancer Res 2014;12:550-9.
31. Huang XP, Li X, Situ MY, et al. Entinostat reverses cisplatin resistance in esophageal squamous cell carcinoma via down-regulation of multidrug resistance gene 1. Cancer Lett 2018;414:294-300.
32. Tang Y, Yang P, Zhu Y, et al. LncRNA TUG1 contributes to ESCC progression via regulating miR-148a-3p/MCL-1/Wnt/β-catenin axis in vitro. Thorac Cancer 2020;11:82-94.
33. Lee KM, Giltnane JM, Balko JM, et al. MYC and MCL1 Cooperatively Promote Chemotherapy-Resistant Breast Cancer Stem Cells via Regulation of Mitochondrial Oxidative Phosphorylation. Cell Metab 2017;26:633-647.e7.
34. Sugase T, Takahashi T, Serada S, et al. SOCS1 Gene Therapy Improves Radiosensitivity and Enhances Irradiation-Induced DNA Damage in Esophageal Squamous Cell Carcinoma. Cancer Res 2017;77:6975-86.
35. Kozopas KM, Yang T, Buchan HL, et al. MCL1, a gene expressed in programmed myeloid cell differentiation, has sequence similarity to BCL2. Proc Natl Acad Sci U S A 1993;90:3516-20.
36. de Melo Silva AJ, de Melo Gama JE, de Oliveira SA. The Role of Bcl-2 Family Proteins and Sorafenib Resistance in Hepatocellular Carcinoma. Int J Cell Biol 2024;2024:4972523.
37. Dakkak BE, Taneera J, El-Huneidi W, et al. Unlocking the Therapeutic Potential of BCL-2 Associated Protein Family: Exploring BCL-2 Inhibitors in Cancer Therapy. Biomol Ther (Seoul) 2024;32:267-80.
38. Thomas LW, Lam C, Edwards SW. Mcl-1; the molecular regulation of protein function. FEBS Lett 2010;584:2981-9.
39. Yang T, Kozopas KM, Craig RW. The intracellular

distribution and pattern of expression of Mcl-1 overlap with, but are not identical to, those of Bcl-2. J Cell Biol 1995;128:1173-84.
40. Peperzak V, Vikström I, Walker J, et al. Mcl-1 is essential for the survival of plasma cells. Nat Immunol 2013;14:290-7.
41. Hoogenboezem EN, Patel SS, Lo JH, et al. Structural optimization of siRNA conjugates for albumin binding achieves effective MCL1-directed cancer therapy. Nat Commun 2024;15:1581.
42. Sun W, Cai H, Zhang K, et al. Targeting MCL1 with Sanggenon C overcomes MCL1-driven adaptive chemoresistance via dysregulation of autophagy and endoplasmic reticulum stress in cervical cancer. Phytomedicine 2024;133:155935.
43. Jamil S, Sobouti R, Hojabrpour P, et al. A proteolytic fragment of Mcl-1 exhibits nuclear localization and regulates cell growth by interaction with Cdk1. Biochem J 2005;387:659-67.
44. Jamil S, Mojtabavi S, Hojabrpour P, et al. An essential role for MCL-1 in ATR-mediated CHK1 phosphorylation. Mol Biol Cell 2008;19:3212-20.
45. Wang H, Guo M, Wei H, et al. Targeting MCL-1 in cancer: current status and perspectives. J Hematol Oncol 2021;14:67.
46. Fultang N, Schwab AM, McAneny-Droz S, et al. PBRM1 loss is associated with increased sensitivity to MCL1 and CDK9 inhibition in clear cell renal cancer. Front Oncol 2024;14:1343004.
47. Terasaki T, Semba Y, Sasaki K, et al. The RNA helicases DDX19A/B modulate selinexor sensitivity by regulating MCL1 mRNA nuclear export in leukemia cells. Leukemia 2024;38:1918-28.
48. Wu X, Iwatsuki M, Takaki M, et al. FBXW7 regulates the sensitivity of imatinib in gastrointestinal stromal tumors by targeting MCL1. Gastric Cancer 2024;27:235-47.
49. Maji S, Samal SK, Pattanaik L, et al. Mcl-1 is an important therapeutic target for oral squamous cell carcinomas. Oncotarget 2015;6:16623-37.
50. Kotschy A, Szlavik Z, Murray J, et al. The MCL1 inhibitor S63845 is tolerable and effective in diverse cancer models. Nature 2016;538:477-82.
51. Liu T, Lam V, Thieme E, et al. Pharmacologic Targeting of Mcl-1 Induces Mitochondrial Dysfunction and Apoptosis in B-Cell Lymphoma Cells in a TP53- and BAX-Dependent Manner. Clin Cancer Res 2021;27:4910-22.
52. Senichkin VV, Streletskaia AY, Gorbunova AS, et al. Saga of Mcl-1: regulation from transcription to degradation. Cell Death Differ 2020;27:405-19.
53. Kuleshov MV, Diaz JEL, Flamholz ZN, et al. modEnrichr: a suite of gene set enrichment analysis tools for model organisms. Nucleic Acids Res 2019;47:W183-90.
54. Subramanian A, Tamayo P, Mootha VK, et al. Gene set enrichment analysis: a knowledge-based approach for interpreting genome-wide expression profiles. Proc Natl Acad Sci U S A 2005;102:15545-50.
55. Kanehisa M, Goto S. KEGG: kyoto encyclopedia of genes and genomes. Nucleic Acids Res 2000;28:27-30.
56. Szklarczyk D, Morris JH, Cook H, et al. The STRING database in 2017: quality-controlled protein-protein association networks, made broadly accessible. Nucleic Acids Res 2017;45:D362-8.
57. Herreros-Villanueva M, Zhang JS, Koenig A, et al. SOX2 promotes dedifferentiation and imparts stem cell-like features to pancreatic cancer cells. Oncogenesis 2013;2:e61.
58. Zhang Y, Chen S, Wei C, et al. Dietary compound proanthocyanidins from Chinese bayberry (Myrica rubra Sieb. et Zucc.) leaves attenuate chemotherapy-resistant ovarian cancer stem cell traits via targeting the Wnt/beta-catenin signaling pathway and inducing G1 cell cycle arrest. Food & Function 2018;9:525-33.
59. Erdogan S, Turkekul K, Dibirdik I, et al. Midkine downregulation increases the efficacy of quercetin on prostate cancer stem cell survival and migration through PI3K/AKT and MAPK/ERK pathway. Biomed Pharmacother 2018;107:793-805.
60. Hu MT, Wang JH, Yu Y, et al. Tumor suppressor LKB1 inhibits the progression of gallbladder carcinoma and predicts the prognosis of patients with this malignancy. Int J Oncol 2018;53:1215-26.

Cite this article as: Chen J, Chen G, Fang X, Sun J, Song J, Chen Z. Elevated *MCL1* expression drives esophageal squamous cell carcinoma stemness and induces resistance to radiotherapy. J Thorac Dis 2024;16(12):8684-8698. doi: 10.21037/jtd-2024-2027